ELSEVIER

www.elsevier.nl/locate/jorganchem

Journal of Organometallic Chemistry 587 (1999) 9–17

Journal of Organometallic Chemistry

Bis-(1,2-*N*,*N*-dimethylaminomethylferrocenyl)dichlorosilane —structure and reactivity

Wolfram Palitzsch [a], Claus Pietzsch [b], Mark Puttnat [c], Klaus Jacob [c], Kurt Merzweiler [d], Piero Zanello [e], Arnaldo Cinquantini [e], Marco Fontani [e], Gerhard Roewer [a,*]

[a] *Institut für Anorganische Chemie, Technische Universität Bergakademie Freiberg, Leipziger Straße 29, D-09596 Freiberg/Sa., Germany*
[b] *Institut für Angewandte Physik, Technische Universität Bergakademie Freiberg, Bernhard von Cotta Straße 4, D-09596 Freiberg/Sa., Germany*
[c] *Institute für Anorganische Chemie der Martin-Luther-Universität Halle–Wittenberg, Geusaer Straße, D-06217 Merseburg, Germany*
[d] *Institute für Anorganische Chemie der Martin-Luther-Universität Halle–Wittenberg, Kurt-Mothes-Straße, D-06120 Halle, Germany*
[e] *Dipartimento di Chimica dell'Universita di Siena, Pian die Mantellini, I-53100 Siena, Italy*

Received 15 March 1999; received in revised form 24 April 1999

Dedicated to: Professor Karl-Heinz Thiele on the occasion of his 70th birthday.

Abstract

The treatment of silicon tetrachloride with two equivalents of 2-dimethyl-aminomethylferrocenyl lithium (**1**), (FcN)Li, affords (*R*,*S*)-$(FcN)_2SiCl_2$ (**3**). Complex **3** was used as the starting chlorosilyl compound for reaction with MeMgCl to give (*R*,*S*)-$(FcN)_2SiMe_2$ (**4**). Dimethyldichlorosilane reacts with two equivalents of **1** to form an isomeric mixture of **4** (*meso*) and (*R*,*R*-) and (*S*,*S*)-bis-(1,2-*N*,*N*-dimethylaminomethylferrocenyl)dimethylsilane. A detailed characterization of **3** and **4** has been carried out by ^{1}H-, ^{13}C-, ^{29}Si-NMR and Mössbauer spectroscopies. The structures of **3** and **4** have been determined by X-ray diffraction analysis. The redox behaviour of **3** and **4** has been studied by electrochemical techniques.

Keywords: Crystal structure; 1,2-*N*,*N*-Dimethylaminomethylferrocenyl; Iron; Mössbauer spectroscopy; Optical activity; Silicon

1. Introduction

The 1,2-*N*,*N*-dimethylaminomethylferrocenyl species (FcN) has been become quite a useful ligand over the past several years [1]. There are now well-established methods for the preparation of transition metal substituted FcN derivatives, but the homologous complexes that are related by a formal substitution of the transition metal by SiR_3 have, so far, attracted little attention. Various FcN silanes have been prepared up to now [2]. Furthermore, it is interesting to study the controlled hydrolysis and condensations of such chlorosilanes as model compounds. Auner and coworkers reported that the intramolecular donor capabilities of the dimethylaminobenzyl ligand at the silicon atom increases the stabilization of 1,3-siloxanedioles [3]. In this manner (FcN)–chlorosilane complexes are interesting synthons to get silanoles. They should also react with different nucleophilic reagents such as complexes of transition metals to create transition metal silicon bonds or with alkali metal silicon compounds to build Si–Si bonds, respectively.

Studies of planar chiral ferrocenes have proven a great challenge in various fields of chemistry [4]. We report here the preparation and characterization of (*R*,*S*)-$(FcN)_2SiCl_2$ (**3**). Its structural data have also been obtained. Furthermore, we demonstrate that it is even possible to prepare (*R*,*S*)-$(FcN)_2SiMe_2$ (**4**) using (*R*,*S*)-$(FcN)_2SiCl_2$ (**3**) as a starting material.

* Corresponding author. Tel.: +49-3731-39-3174; fax: +49-3731-39-4058.
E-mail address: roewer@orion.hrz.tu-freiberg.de (G. Roewer)

0022-328X/99/$ - see front matter
PII: S0022-328X(99)00244-2

2. Results and discussion

The treatment of silicon tetrachloride with two equivalents of (FcN)Li (**1**) in DME results in the formation of $(FcN)_2SiCl_2$ (**3**) as a reddish solid (Scheme 1).

Recrystallization from pentane at −20°C gave analytically pure orange–red crystals of **3** suitable for X-ray crystallographic study (Fig. 1). The iron atom in this compound shows a similar coordination geometry to that found in $(FcN)SiCl_3$ (**2**) [5]. The FcN fragment adopts an eclipsed conformation. Unfortunately there is no evidence for an interaction between the nitrogen atoms and the silicon atom. Within the limits of experimental error, all the corresponding C–C and C–Fe distances in the ferrocene fragment of **3** are identical and they have expected values. The bond lengths Si–Cl1

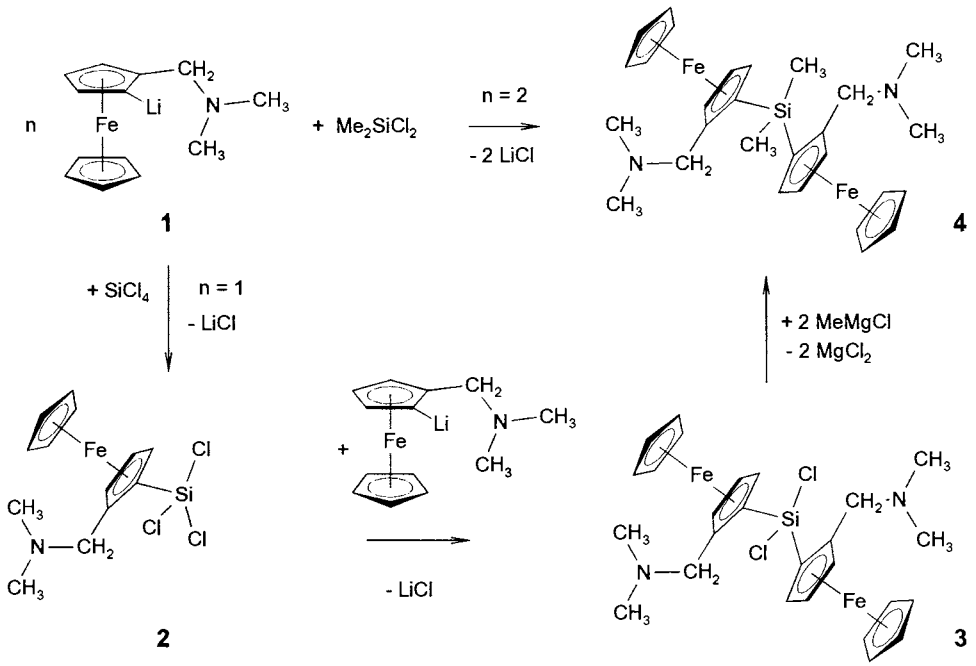

Scheme 1.

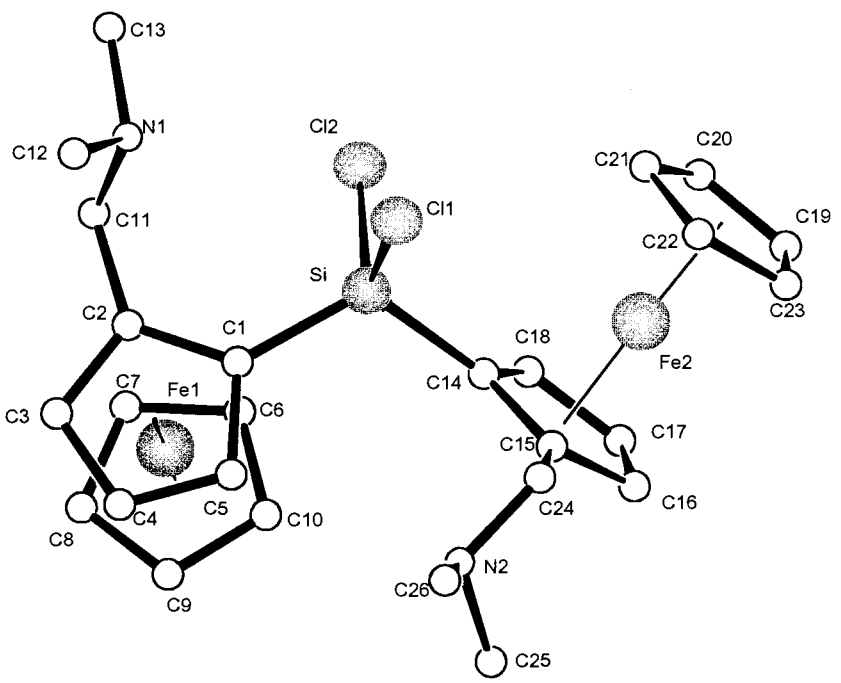

Fig. 1. Molecular structure of **3**. Hydrogen atoms are omitted for clarity.

Table 1
Formal electrode potentials (V vs. SCE) and peak-to-peak separations (mV) for the oxidation processes exhibited by the silicon–ferrocene complex **3** under study

Complex	Oxidation processes			Solvent
	$E^{\circ\prime}$	ΔE_p [a]	$E^{\circ\prime}$	
$(FcN)_2SiCl_2$	+0.52 [b]		+0.64 [f]	MeCN [d]
FcNH	+0.36 [e]	67		MeCN [d]
	+0.38 [e]	122		CH_2Cl_2 [c]

[a] Measured at 0.2 V s^{-1}.
[b] First one-electron oxidation.
[c] Second one-electron oxidation.
[d] $[NEt_4][ClO_4]$ 0.1 mol dm^{-3} supporting electrolyte.
[e] One-electron process.
[f] $[NBu_4][PF_6]$ 0.2 mol dm^{-3} supporting electrolyte.

Table 2
Crystallographic data and experimental parameters for compound **3** and **4**

Compound	$(FcN)_2SiCl_2$ (**3**)	$(FcN)_2SiMe_2$ (**4**)
Empirical formula	$C_{26}H_{32}Cl_2Fe_2N_2Si$	$C_{28}H_{38}Fe_2N_2Si$
Formula weight (g mol^{-1})	583.23	542.39
Crystal system	Monoclinic	Orthorhombic
Space group	$P2_1/c$	*Pbca*
Z	4	8
a (Å)	8.3899(11)	8.150(2)
b (Å)	24.908(2)	20.363(6)
c (Å)	12.906(2)	32.840(6)
β (°)	97.241(14)	90
V (Å^3)	2675.4(3)	5450(2)
$D_{calc.}$ (Mg m^{-3})	1.448	1.322
Absorption coeff. (mm^{-1})	1.346	1.127
$F(000)$	1208	2288
θ range (°)	2.58 to 27.11	2.00 to 24.05
Reflections	5763	4244
R_{int}	0.0546	0.0649
Data/parameters	5759/426	4244/450
Goodness-of-fit on F^2	1.060	0.994
$R_1/wR_2[I = 2\sigma(I)]$	0.0358/0.0841	0.0364/0.0792
R_1/wR_2 (all data)	0.0455/0.092	0.0574/0.0854
Largest diff. peak and hole (e Å^3)	0.465/−0.508	0.490/−0.224

(205.3 pm) and Si–Cl_2 (205.7 pm) do not exhibit any anomalies (see Tables 3 and 5). By careful evaluation of the results of the X-ray crystallographic study we found that the orange–red crystals of **3** embody the (*R*,*S*)-FcN_2SiCl_2 (*meso*) which represents only one member of the expected diastereomer set. In order to isolate the (*R*,*R*)- and (*S*,*S*)-FcN_2SiCl_2 we also analyzed the mother liquor, but unfortunately we were not able to find any trace of a racemate.

The ^{1}H- and ^{13}C-NMR spectra for complex **3** exhibit in each case peaks of the FcN unit only (see Table 7). In the ^{1}H-NMR spectrum the typical signals of the FcN ligands are located at 2.09 (s, –$N(CH_3)_2$), 2.94, 2.91, 3.77, 3.74 (AB, CH_2–N), 4.00 (s, C_5H_5) and 4.40, 4.43, 4.46 ppm as multiplets that indicate the protons of the substituted cyclopentadienyl group. Methylene group protons give significantly different chemical shift values. The recorded non-equivalence of methylene group protons in 1,2-disubstituted ferrocenes agrees with results given in previous papers [6]. ^{13}C-NMR data of **3** confirm the proposed structure (Table 7). The ^{29}Si-NMR signal of the $SiCl_2$ group appears at 14.02 ppm.

The treatment of a solution of (*R*,*S*)-FcN_2SiCl_2 (**3**) in diethylether with a solution of MeMgCl in diethylether affords the pure (*R*,*S*)-FcN_2SiMe_2 (**4**, Scheme 1). Evidence is given by the X-ray cyrstallographic analysis. Recrystallization from pentane at −20°C gave analytically pure red crystals of **4** suitable for X-ray crystallographic study (Fig. 2). The structural features of **4** seem to be normal [5]. Crystallographic data and data collection parameters are listed in Table 2. Important bond distances and angles are listed in Table 4 (see also Table 6).

The ^{1}H-NMR signal for the methyl groups (SiMe) is situated at 0.68 ppm. Additionally the ^{1}H-NMR spectrum exhibits typical peaks for the FcN ligand at 1.96 (s, –$N(CH_3)_2$), 3.07, 3.10, 3.34, 3.37 (AB, CH_2–N), 4.09 (s, C_5H_5) and in the range from 4.17 to 4.30 ppm as multiplets of the protons of the substituted cyclopentadienyl ring of the ferrocenyl system. The resonance of the silicon atom is found at $\delta = -7.62$ ppm in ^{29}Si-NMR. The assigned structure was proven by the ^{13}C-NMR spectrum (see Table 7). Data are in accordance with Fig. 2.

Our results suggest that we should be able to control the synthesis conditions in such a way that only the (*R*,*S*)-FcN_2SiMe_2 isomer of **4** will be formed immediately. So we were very keen on checking an alternative preparation route of **4**. The reaction of two equivalents of FcNLi (**1**) with Me_2SiCl_2 in THF at ambient temperature should give FcN_2SiMe_2 (**4**) (Scheme 1) [7]. Our result is contrary to former works where **4** was reported as 'simple' FcN_2SiMe_2 [6,7]. It should be pointed out that the ^{1}H-NMR spectrum of the orange solid received consists of two sets of signals. We observed a doubling of all signals in the NMR spectra. The methyl groups introduced on the silicon atom are indicated as a set of two singulets at 1.83 and 1.79 ppm in the ^{1}H-NMR spectrum. The ^{29}Si-NMR spectrum shows two signals for the $SiMe_2$ group (−7.62 and −6.06 ppm). Presumably our product is representing a mixture of *meso*-FcN_2SiMe_2, (*R*,*R*)-FcN_2SiMe_2 and (*S*,*S*)-FcN_2SiMe_2 isomers (Fig. 3). We were not able to separate *meso*-FcN_2SiMe_2 from (*R*,*R*)- and (*S*,*S*)-FcN_2SiMe_2 by column chromatography, but fractionated recrystallization gave the *meso* compound separately. From comparison between the NMR spectra of the precipitated crystals and of the solid received from the mother liquor, we conclude that an isolation of stereochemi-

Table 3
Selected bond lengths and angles for **3**

Bond lengths (Å)					
Cl1–Si	2.053(1)	Fe1–C9	2.022(2)	Fe2–C17	2.051(2)
Si–C1	1.829(2)	Fe1–C10	2.021(4)	Fe2–C18	2.036(2)
Fe1–C1	2.029(2)	N1–C11	1.448(3)	Fe2–C19	2.045(3)
Fe1–C2	2.036(2)	N1–C12	1.429(4)	Fe2–C20	2.044(3)
Fe1–C3	2.052(3)	N1–C13	1.454(3)	Fe2–C21	2.030(3)
Fe1–C4	2.055(3)	Cl2–Si	2.057(2)	Fe2–C22	2.026(3)
Fe1–C5	2.036(2)	Si–C14	1.838(2)	Fe2–C23	2.040(3)
Fe1–C6	2.043(4)	Fe2–C14	2.044(2)	N2–C24	1.456(3)
Fe1–C7	2.033(4)	Fe2–C15	2.031(2)	N2–C25	1.437(5)
Fe1–C8	2.037(3)	Fe2–C16	2.036(2)	N2–C26	1.459(4)
Bond angles (°)					
C1–Si–C14	115.2(1)	C14–Si–Cl1	110.2(1)	C14–Si–Cl2	105.9(1)
C1–Si–Cl1	107.5(1)	C1–Si–Cl2	111.2(1)	Cl1–Si–Cl2	106.6(1)

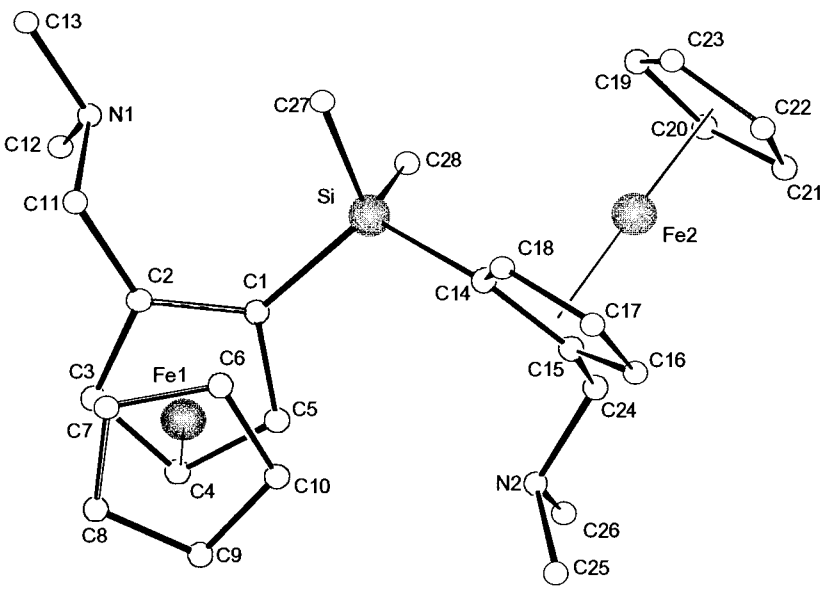

Fig. 2. Molecular structure of **4**. Hydrogen atoms are omitted for clarity.

Table 4
Selected bond lengths and angles for **4**

Bond lengths (Å)					
C1–Si	1.867(3)	Fe1–C9	2.038(4)	Fe2–C17	2.053(3)
Si–C27	1.856(4)	Fe1–C10	2.034(4)	Fe2–C18	2.041(3)
Si–C28	1.876(4)	N1–C11	1.459(4)	Fe2–C19	2.042(3)
C14–Si	1.874(3)	N1–C12	1.441(5)	Fe2–C20	2.040(4)
Fe1–C3	2.040(4)	N1–C13	1.460(4)	Fe2–C21	2.038(5)
Fe1–C4	2.038(4)	Fe1–C1	2.056(3)	Fe2–C22	2.033(4)
Fe1–C5	2.035(3)	Fe1–C2	2.043(3)	Fe2–C23	2.039(4)
Fe1–C6	2.026(5)	Fe2–C14	2.061(3)	N2–C24	1.460(4)
Fe1–C7	2.028(4)	Fe2–C15	2.018(3)	N2–C25	1.436(6)
Fe1–C8	2.035(3)	Fe2–C16	2.026(3)	N2–C26	1.440(5)
Bond angles (°)					
C1–Si–C14	110.7(1)	C14–Si–C28	107.1(2)	C14–Si–C27	112.8(2)
C1–Si–C28	111.6(2)	C1–Si–C27	105.2(2)	C27–Si–C28	109.6(3)

Table 5
Atomic coordinates ($\times 10^4$) and equivalent isotropic displacement parameters ($A^2 \times 10^3$) for **3** [a]

	x	y	z	U_{eq}
C(1)	−2972(2)	4169(1)	2568(2)	36(1)
C(2)	−3684(3)	4466(1)	3346(2)	41(1)
C(3)	−4776(3)	4841(1)	2813(2)	55(1)
C(4)	−4749(4)	4784(1)	1731(2)	60(1)
C(5)	−3643(3)	4373(1)	1565(2)	46(1)
C(6)	−92(5)	5084(2)	2896(5)	92(1)
C(7)	−1002(6)	5453(2)	3397(4)	94(1)
C(8)	−1942(6)	5757(1)	2649(5)	102(1)
C(9)	−1598(9)	5581(2)	1689(5)	122(2)
C(10)	−468(7)	5160(2)	1840(5)	115(2)
C(11)	−3370(3)	4387(1)	4503(2)	47(1)
C(12)	−5471(5)	3743(3)	4564(4)	99(2)
C(13)	−3257(5)	3746(2)	5892(2)	65(1)
C(14)	−174(2)	3592(1)	1675(2)	32(1)
C(15)	−423(2)	3371(1)	633(2)	36(1)
C(16)	1033(3)	3430(1)	187(2)	44(1)
C(17)	2190(3)	3680(1)	921(2)	47(1)
C(18)	1464(3)	3779(1)	1832(2)	40(1)
C(19)	3291(3)	2458(1)	1694(3)	62(1)
C(20)	2829(4)	2584(1)	2664(2)	69(1)
C(21)	1242(5)	2430(2)	2657(3)	79(1)
C(22)	708(4)	2206(1)	1671(4)	83(1)
C(23)	1996(4)	2227(1)	1072(3)	67(1)
C(24)	−1934(3)	3129(1)	82(2)	43(1)
C(25)	−2438(5)	3834(2)	−1174(3)	88(1)
C(26)	−4570(4)	3268(2)	−798(3)	82(1)
N(1)	−3789(3)	3848(1)	4794(2)	51(1)
N(2)	−3075(2)	3530(1)	−373(2)	51(1)
Fe(1)	−2490(1)	4964(1)	2456(1)	50(1)
Fe(2)	1392(1)	2979(1)	1511(1)	36(1)
Si	−1498(1)	3625(1)	2704(1)	33(1)
Cl(1)	−2740(1)	2917(1)	2763(1)	55(1)
Cl(2)	−3(1)	3683(1)	4091(1)	54(1)

[a] U_{eq} is defined as one third of the trace of the orthogonalized U_{ij} tensor.

cally pure (*R*,*S*)-FcN_2SiMe_2 (**4**) was realized from the mixture of its diastereomers (Fig. 4).

3. Electrochemistry

Fig. 5 shows the voltammetric pattern exhibited by $(FcN)_2SiCl_2$ (**3**) in acetonitrile solution.

Two essentially overlapping oxidation processes are present, which because of a slight adsorption phenomena, are not well separated even in differential pulse voltammetry. Controlled potential coulometry in correspondence to the second step ($E_w = +0.7$ V) consumes two electrons per molecule and the subsequent cyclic voltammetry confirms the chemical reversibility of the overall two-electron removal. Since the oxidized solution assumes a green colour ($\lambda_{max} = 634$ nm), it is conceivable that the HOMO represents a d-orbital of iron. The occurrence of two almost overlapping oxidation steps ($\Delta E^{\circ\prime} = 0.12$ V) [8] suggests a weak electronic communication between the ferrocene subunits, as it occurs on the other hand for $FcSi(Me)_2Fc$ in some solvents [9]. But the comparison with $(Fc)_3SiCl$ (unpublished work) seems to support the fact that the presence of dimethylaminomethyl substituents in the ferrocene units tends to enhance the communication of the multiple redox-active centers among the redox sites. This means the communication among the redox sites is governed not only by the nature of the bridging moieties but also by the intrinsic donor–acceptor ability of the redox-active subunits themselves [10]. The electrochemical parameters for compound **3** are summarized in Table 1.

A complex oxidation mechanism is involved in the oxidation of the diferrocenyl–silicon complex **4**. Fig. 6(a) shows that it undergoes two main oxidation processes, the first one being irreversible ($E_p = +0.33$ V at 0.2 V s^{-1}), whereas the second one is reversible. A third minor oxidation process is also present. Indeed, as Fig. 6(b) shows, the second step consists of two almost

Table 6
Atomic coordinates ($\times 10^4$) and equivalent isotropic displacement parameters ($A^2 \times 10^3$) for **4** [a]

	x	y	z	U_{eq}
C(1)	6466(4)	7181(1)	3831(1)	43(1)
C(2)	7228(4)	6543(1)	3809(1)	49(1)
C(3)	8227(5)	6458(2)	4158(1)	58(1)
C(4)	8113(5)	7026(2)	4400(1)	61(1)
C(5)	7050(4)	7469(2)	4203(1)	53(1)
C(6)	3436(6)	6382(2)	4298(2)	84(1)
C(7)	4381(6)	5819(2)	4391(2)	85(2)
C(8)	5193(6)	5934(2)	4749(1)	82(1)
C(9)	4775(7)	6568(2)	4886(1)	84(1)
C(10)	3691(6)	6845(2)	4603(1)	83(1)
C(11)	7057(5)	6042(2)	3474(1)	54(1)
C(12)	9524(6)	6402(3)	3135(2)	92(2)
C(13)	7570(7)	5750(2)	2778(1)	76(1)
C(14)	3569(4)	8138(1)	3738(1)	43(1)
C(15)	3615(4)	8760(1)	3948(1)	48(1)
C(16)	2027(5)	8898(2)	4094(1)	58(1)
C(17)	969(5)	8391(2)	3981(1)	59(1)
C(18)	1898(4)	7933(2)	3765(1)	55(1)
C(19)	2461(6)	8877(3)	2868(1)	84(1)
C(20)	2960(7)	9447(3)	3054(2)	89(2)
C(21)	1584(8)	9729(3)	3242(2)	95(2)
C(22)	267(7)	9323(3)	3168(2)	93(2)
C(23)	796(6)	8790(3)	2938(1)	89(1)
C(24)	5052(5)	9212(2)	4004(1)	58(1)
C(25)	5207(8)	9052(3)	4729(1)	98(2)
C(26)	7458(7)	9496(2)	4367(2)	88(2)
C(27)	6597(6)	8156(3)	3164(2)	86(2)
C(28)	4027(7)	7071(3)	3112(2)	88(2)
N(1)	7807(4)	6249(1)	3091(1)	60(1)
N(2)	6095(3)	9048(1)	4351(1)	59(1)
Si(1)	5153(1)	7641(1)	3463(1)	49(1)
Fe(1)	5850(1)	6616(1)	4327(1)	52(1)
Fe(2)	2021(1)	8821(1)	3479(1)	51(1)

[a] U_{eq} is defined as one third of the trace of the orthogonalized U_{ij} tensor.

Table 7
^{1}H-, ^{13}C- and ^{29}Si-NMR data of the derivatives **3** and **4** [a]

Compound	δ ^{1}H		δ ^{13}C		δ ^{29}Si
	FcN	Me–Si	Me–Si	FcN	
3	2.09 (s 6H); 4.00 (s 5H); 2.91, 2.94, 3.74, 3.77 (AB CH_2–N); 4.40, 4.43, 4.46 (m 3H)			91.04; 76.00, 73.40; 70.97; 70.19; 69.52; 58.21; 44.08	14.02
(*R*,*S*)-**4**	1.96 (s 12H); 4.09 (s 10H); 3.07, 3.10, 3.34, 3.37 (AB CH_2–N);4.17, 4.18, 4.30, (m 6H)	0.68 (s 6H)	0.13	90.03; 75.40; 72.98; 71.61; 69.17; 68.90; 59.58; 44.97	−7.62
(*R*,*R*)-/(*S*,*S*)-**4**	2.15 (s); 4.05 (s); 3.00, 3.03, 3.42, 3.46 (AB CH_2–N);4.12, 4.22, 4.35 (m)	0.70, 0.56	1.08, 0.35	90.29; 75.36; 73.23; 72.06; 69.37; 68.84; 59.83; 45.35	−6.06

[a] At 25°C data in ppm are relative to Me_4Si at 0.0 ppm; recorded in $CDCl_3$.

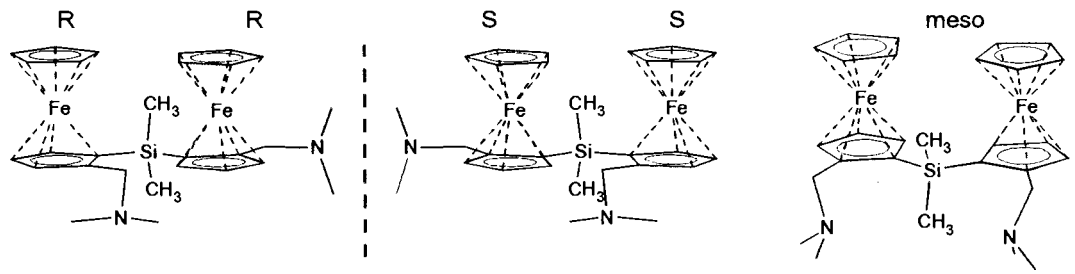

Fig. 3. *meso*-FcN_2SiMe_2, (*R*,*R*)-FcN_2SiMe_2 and (*S*,*S*)-FcN_2SiMe_2

overlapping processes. At high scan rate, Fig. 6(c), the chemical complications following the first one-electron removal are almost completely prevented and only the two first anodic steps take place ($E^{\circ\prime} = +0.32$ V and $+0.53$ V, respectively). Finally, Fig. 6(d) shows the cyclic voltammogram recorded after a cycle of exhaustive oxidation/exhaustive rereduction.

Two new reversible peak systems are present at $E^{\circ\prime} = +0.56$ and $+0.76$ V, respectively. The most straightforward explanation of the oxidation mechanism is the following one: the anodic oxidation of **4** proceeds through two separated one-electron oxidations, which at low scan rates, as a consequence of the coupled chemical complications, give rise in cyclic voltammetry to traces of two new peaks at higher potential values. As a matter of fact, exhaustive oxidation completely converts **4** to the species responsible for these new peaks, the most anodic one being affected by adsorption phenomena. By way of speculation, we point out that $(FcN)_2SiMe_2$ in dichloromethane solution displays two separated reversible one-electron oxidations at potential values essentially identical to the new peak-systems shown in Fig. 6(d) [11]. As seen, the presence of the silicon fragments tends to make the oxidation of the ferrocene subunit(s) more difficult with respect to ferrocene as well as dimethylaminomethylferrocene free ligands, thus proving that these silicon substituents withdraw significant electron density from the ferrocene unit(s).

4. Mössbauer spectroscopy

The Mössbauer spectra were recorded at 100 K absorber temperature. Table 8 contains the results of these measurements. The spectra show the same pattern (Fig. 7). The doublet is created by iron(II) in the ferrocene skeleton. The measurements have shown that in compounds including ferrocenyl groups bridged by chlorosilyl groups does not exist any communication among the two iron centers. The singlet which was found for compound **4** additionally holds for iron (III). We assume that a weak intervalence electron transfer for the Fe (III) part of the spectrum between the iron atoms in both ferrocenyle systems about the silicon chain of compound **4** is responsible [5].

5. Experimental

5.1. General

All manipulations involving air- and moisture-sensitive organometallic compounds were carried out by the use of the standard Schlenk and glove-box techniques

under an argon atmosphere. All solvents were freshly distilled, degassed and dried prior to use. Synthesis of (FcN)Li [12] was carried out according to known procedures. All other reagents were commercial products and were used without further purification.

NMR spectra were recorded on Bruker MSL 200 and Varian Gemini XL-300. UV spectra were measured on Specord M 40 instrument. Mass spectra were measured on a Sector-Field-Mass-Spectrometer AMD 402. Mössbauer spectra were recorded on a Wissel system at 100 K, using a 1.8 GBq ^{57}Co source in a rhodium matrix (isomer shift relative to α_{Fe}).

5.2. Synthesis of complexes **3** and **4**

5.2.1. Preparation of $(FcN)_2SiCl_2$ (**3**)

[2-(dimethylaminomethyl)ferrocenyl]-lithium(24mmol, 6 g) was dissolved in DME and added slowly, over a period of 4 h, to a solution of $SiCl_4$ (12 mmol, 2 g) in pentane. The reaction mixture was stirred for an additional 3 h before the solvents and unreacted $SiCl_4$ were removed under vacuum. The resulting orange solid was recrystallized from pentane after removing LiCl. This purification leads to orange–red crystals. Yield: 12 g (86%). Found: C, 52.86; H, 6.57; N, 4.88.

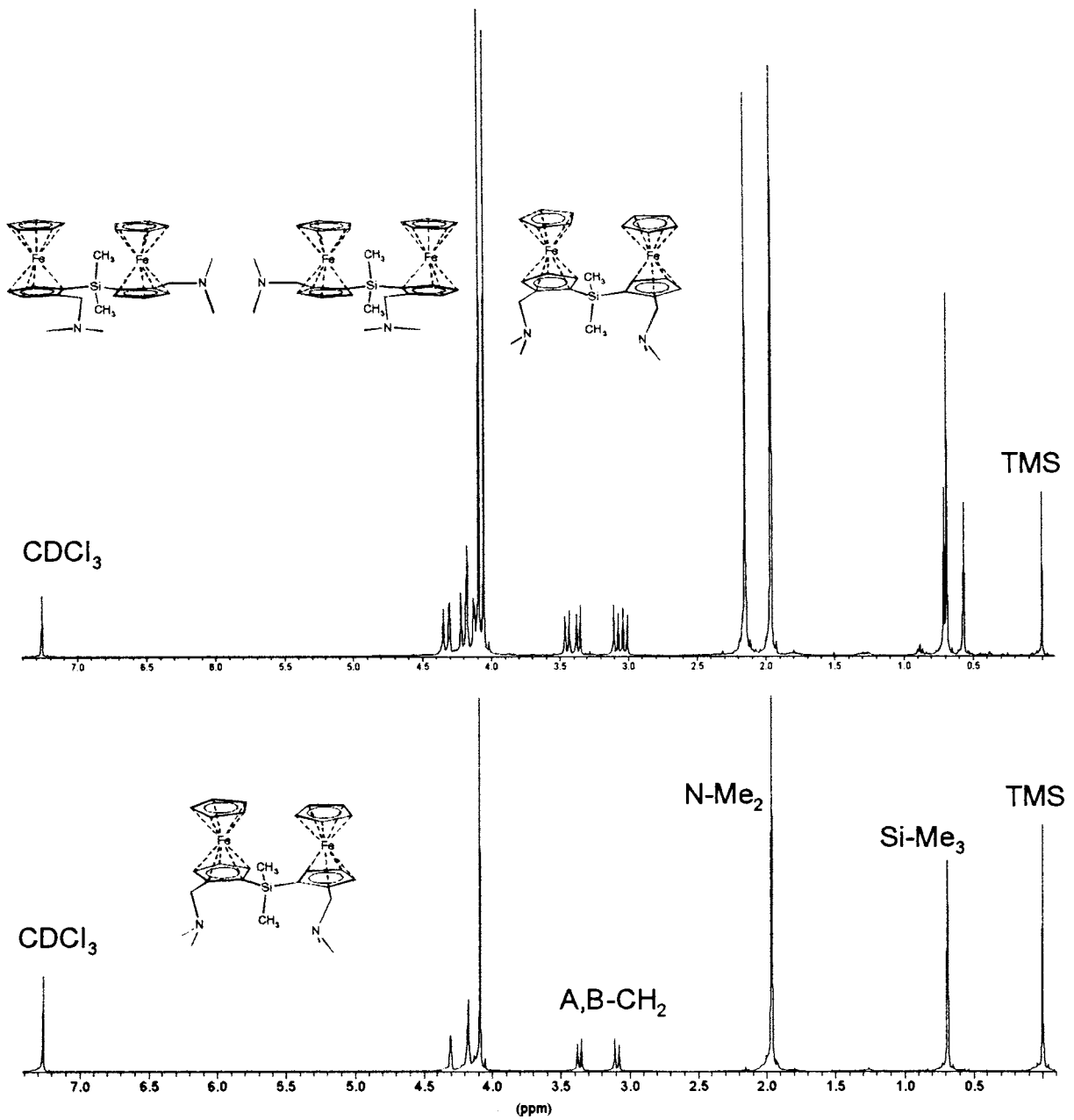

Fig. 4. ^{1}H-NMR spectra of mother liquior (upper part) and solution of separated crystals of **4** (below).

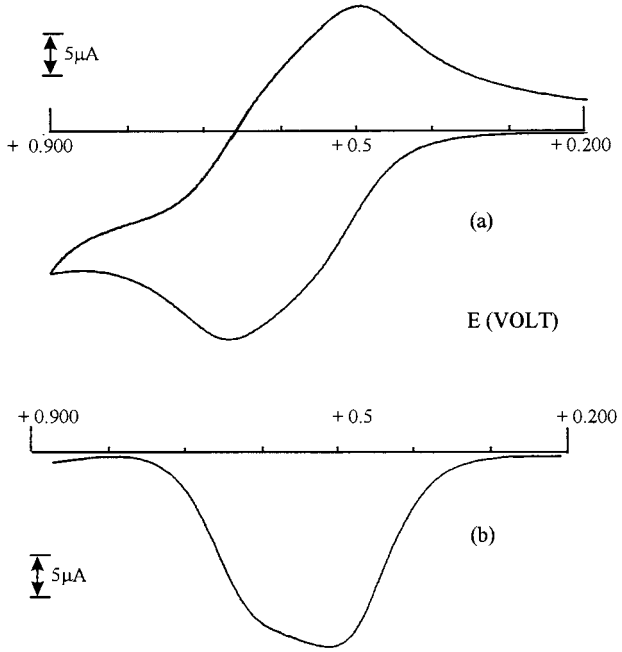

Fig. 5. Cyclic (a) and differential pulse (b) voltammetric responses recorded at a platinum electrode on a MeCN solution containing $(FcN)_2SiCl_2$ (**3**) (6×10^{-4} mol dm^{-3}) and $[NEt_4][ClO_4]$ (0.1 mol dm^{-3}). Scan rates: (a) 0.2 V s^{-1}; (b) 0.004 V s^{-1}.

$C_{26}H_{32}Cl_2Fe_2N_2Si$ (583.23) Anal. Calc.: C, 53.52; H, 6.65; N, 4.80. MS (70 eV) $m/e = 583$ (30%, M^+), 547 (50%, $[(FcN)_2SiCl]^+$), 502 (25%, $[(FcN)SiCl(Fc)CH_2]^+$), 471 (30%, $[(Fc)_2SiCl_2]^+$), 337 (25%, $[(FcN)SiCl_2]^+$), 91 (30%, $[C_5H_4Si]^+$).

Table 8
Mössbauer data of the derivatives **3** and **4** [a]

Compound	δ (mm^{-1})	ε (mm^{-1})	Γ (mm^{-1})	I (%)
3	0.509(3)	2.307(5)	0.30(1)	100(2)
4	0.526(2)	2.362(4)	0.42(9)	92(1)
	0.32(3)		0.42(9)	8(1)

[a] δ = isomer shift (rel. αFe); ε = quadrupole splitting; Γ = line width; I = line area.

5.2.2. Preparation of (R,S)-$(FcN)_2SiMe_2$ (4)

A solution of 2 g (3.4 mmol) of $(FcN)_2SiCl_2$ (**3**) in 50 ml diethyl ether was treated with an exess of a Grignard solution (CH_3MgCl in diethyl ether) at 0°C. The reaction mixture was stirred for 12 h at ambient temperature. The solvent was removed in vacuo and the dark orange product was dissolved with pentane/methanol and filtered. The solvents were removed under reduced pressure and an orange solid (**4**) was obtained. A clear orange solution from pentane was cooled to −20°C overnight to produce crystals. Yield: 1.5 g (81%). Found: C, 60.88; H, 6.89; N, 5.82. $C_{28}H_{38}Fe_2N_2Si$ (542.39) Anal. Calc.: C, 61.95; H, 7.01; N, 5.16. MS (70 eV) $m/e = 542$ (64%, M^+), 256 (15%, $[(Fc–CH_2)SiMe_2]^+$), 255 (10%, $[(FcN)SiMe]^+$), 228 (10%, $[(Fc)SiMe_2]^+$), 242 (100%, $[(FcN)]^+$), 58 (20%, $[SiMe_2]^+$). UV: pentane 326, 451 nm, acetonitrile 325.4, 453 nm.

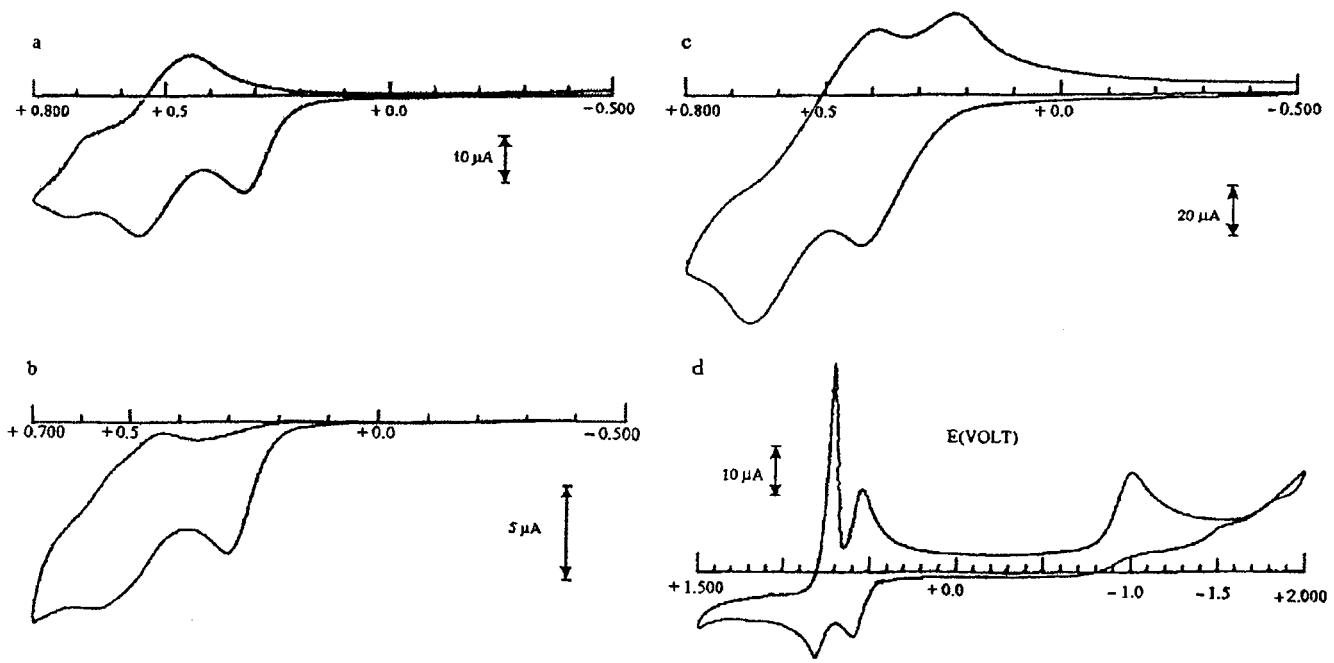

Fig. 6. Cyclic voltammetric responses recorded at a platinum electrode on a CH_2Cl_2 solution containing **4** (1.0×10^{-4} mol dm^{-3}) and $[NBu_4][PF_6]$ (0.2 mol dm^{-3}). Scan rates: (a,d) 0.2 V s^{-1}; (b) 0.02 V s^{-1}; (c) 2.00 V s^{-1}.

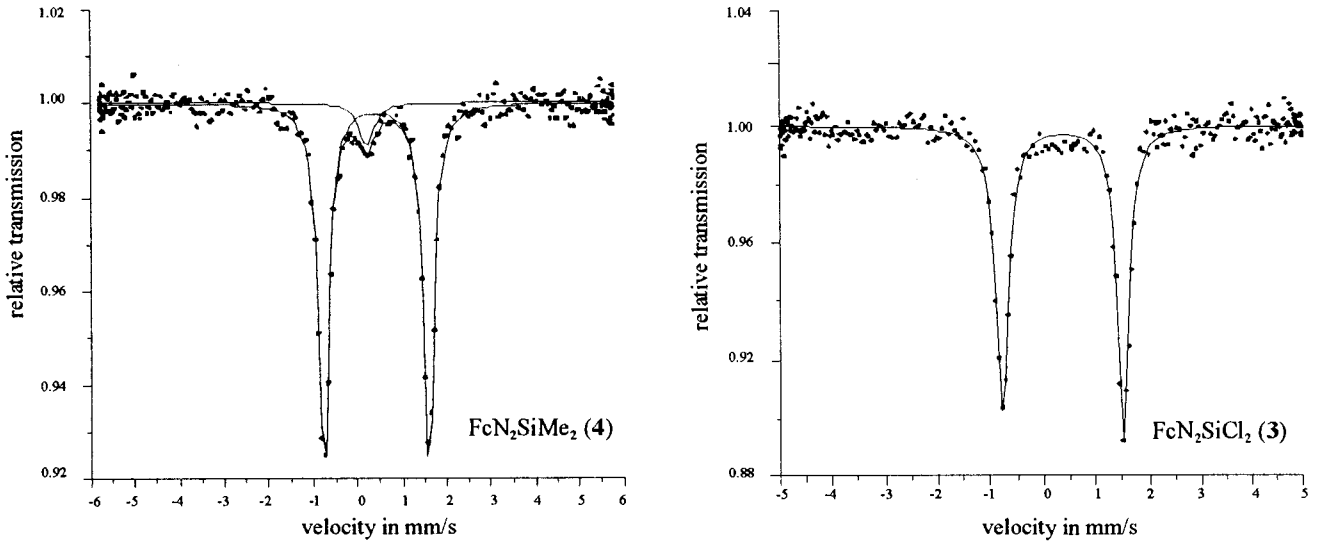

Fig. 7. Mössbauer spectra of compounds **3** and **4**.

6. Supplementary material

Crystallographic data for the structural analysis have been deposited with the Cambridge Crystallographic Data Centre, CCDC 114194 for compound **3** and CCDC 114195 for compound **4**. Copies of this information may be obtained free of charge from: The Director, CCDC, 12 Union Road, Cambridge, CB2 1EZ, UK (Fax: +44-1223-336-033; email: deposit@ccdc.cam.ac.uk or www: http://www.ccdc.cam.ac.uk).

Acknowledgements

Financial support of this work by the Deutsche Forschungsgemeinschaft and the Fond der Chemischen Industrie is gratefully acknowledged. P. Zanello acknowledges the financial support of University of Siena (ex-quota 60%) and the technical assistance of G. Montomoli.

References

[1] F.T. Edelmann, K. Jacob, J. Prakt. Chem. 340 (1998) 393.
[2] A.J. Blake, F.R. Mayers, A.G. Osborne, D.R. Rosseinsky, J. Chem. Soc. Dalton Trans. 12 (1982) 2379.
[3] N. Auner, R. Probst, C.R. Heikenwälder, E. Herdtweck, S. Gamper, G. Müller, Z. Naturforsch. 48b (1993) 1625.
[4] (a) A.D. Ryabov, I.M. Panyashkina, V.A. Polyakov, J.A.K. Howard, L.G. Kuzmina, M.S. Datt, C. Sacht, Organometallics 17 (1998) 3615. (b) A. Togni, Angew. Chem. Int. Ed. Engl. 35 (1996) 1475.
[5] W. Palitzsch, C. Pietzsch, K. Jacob, F.T. Edelmann, Th. Gelbrich, V. Lorenz, M. Puttnat, G. Roewer, J. Organomet. Chem. 554 (1998) 139.
[6] G. Marr, R.E. Moore, B.W. Rockett, Tetrahedron Lett. 21 (1968) 2521.
[7] H.-G. Du, X.-X. Shi, J.-D. Ye, S.-J. Shi, Gaodeng Xuexiao Huaxue Xuebao 18 (10) (1997) 1642.
[8] D.E. Richardson, H. Taube, Inorg. Chem. 20 (1981) 1278.
[9] (a) H. Atzkern, J. Hiermeier, F.H. Kohler, A. Steck, J. Organomet. Chem. 408 (1991) 281. (b) V.V. Dement'ev, F. Cervantes-Lee, L. Parkanyi, H. Sharma, K.H. Pannell, T. Nguyen, A. Diaz, Organometallics 12 (1993) 1983. (c) R. Rulkens, A.J. Lough, I. Manners, S.R. Lovelace, C. Grant, W.E. Geiger, J. Am. Chem. Soc. 118 (1996) 12683.
[10] T. Weyland, C. Lapite, G. Frapper, M.J. Calhorda, J.-F. Halet, L. Toupet, Organometallics 16 (1997) 2024.
[11] V.V. Dement'ev, F. Cervantes-Lee, L. Parkanyi, H. Sharma, K.H. Pannell, M.T. Nguyen, A. Diaz, Organometallics 12 (1993) 1983.
[12] M.D. Rausch, G.A. Moser, C.F. Maede, J. Organomet. Chem. 51 (1973) 1.